

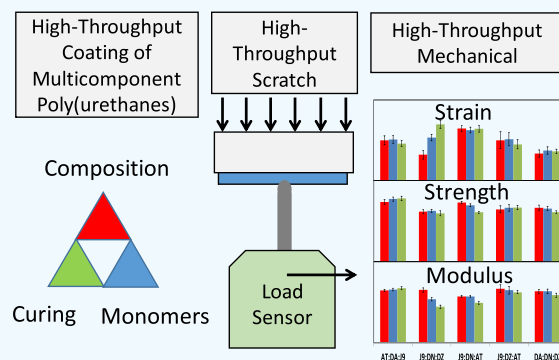
High Throughput Screening of Mechanical Properties and Scratch Resistance of Tricomponent Polyurethane Coatings

Ismael J. Gomez,[†] Jie Wu,[†] John Roper,[§] Haskell Beckham,[‡] and J. Carson Meredith^{*,†,‡,§}[†]School of Chemical and Biomolecular Engineering and [‡]School of Materials Science and Engineering, Georgia Institute of Technology, Atlanta, Georgia 30332, United States[§]Dow Chemical Company, Midland, Michigan 48674, United States

Supporting Information

ABSTRACT: High throughput screening (HTS) is relevant to polymer applications that require rapid screening of limited quantities of material. Polyurethane coating formulations represent one such application because multiple isocyanates or polyols are often blended to achieve specific mechanical and thermal properties. In addition, these formulations often encounter variations in curing conditions in actual use, and a rapid way to assess these variations is desirable. However, exploring the large number of possible combinations of compositions, structure, and curing conditions is experimentally challenging, especially when mechanical and durability properties are desired. We report a comprehensive screening of urethane films by using FTIR-ATR, a high throughput tensile mechanical characterization (HTMECH) apparatus, and a high throughput scratch (HTScratch) characterization method. We synthesized libraries containing three-component films composed of pure or blended polyisocyanates (1,6-hexamethylene diisocyanate or isophorone diisocyanate) and pure or blended polyols (hydroxyl-terminated polyacrylate or a modified acrylic copolymer). The HTS tools were used to explore 36 independent characterizations, performed in triplicate for each of the 57 independent sample conditions (structure, composition, and curing condition), resulting in a total of 2166 unique measurements. The HTS characterization allowed efficient identification of a small subset of systems where the toughness, strain at break, elastic modulus, and scratch resistance could be tuned by adjusting composition and diisocyanate T_g . An interesting feature of the discovery is that the highly tunable systems were only identified under rapid curing conditions, and under slower curing there was less ability to tune the tensile and scratch resistance properties by adjusting composition and precursor T_g .

KEYWORDS: high throughput, combinatorial, polyurethanes, coatings, scratch resistance



We synthesized libraries containing three-component films composed of pure or blended polyisocyanates (1,6-hexamethylene diisocyanate or isophorone diisocyanate) and pure or blended polyols (hydroxyl-terminated polyacrylate or a modified acrylic copolymer). The HTS tools were used to explore 36 independent characterizations, performed in triplicate for each of the 57 independent sample conditions (structure, composition, and curing condition), resulting in a total of 2166 unique measurements. The HTS characterization allowed efficient identification of a small subset of systems where the toughness, strain at break, elastic modulus, and scratch resistance could be tuned by adjusting composition and diisocyanate T_g . An interesting feature of the discovery is that the highly tunable systems were only identified under rapid curing conditions, and under slower curing there was less ability to tune the tensile and scratch resistance properties by adjusting composition and precursor T_g .

INTRODUCTION

Multicomponent polyurethane coatings are an important class of surface protection materials.¹ Polyurethane (PU) coatings can be optimized to provide mechanical strength, gloss, and substrate adhesion leading to their usefulness in marine antifouling,² automotive finishing,^{3,4} and aircraft weathering protection.⁵ Minimization of damage during marring or scratching is essential to preserving the chemical and physical protection of the underlying surface as well as the aesthetic features of coatings. PU elastomers can be prepared as linear polymers when difunctional hydroxyl compounds are reacted with difunctional isocyanate reactants or cross-linked polymers when the functionality of the hydroxyl or isocyanate component is increased to three or more.⁶ Chemical factors, e.g., the urethane linkage and structures of the polyisocyanates and polyols, along with preparation conditions, e.g., isocyanate (NCO):hydroxyl (OH) ratios, curing humidity, curing temperature, etc., greatly influence such PU end properties as heat resistance, chemical resistance, weather resistance, tensile strength, and elongation.⁷ The ability to control these

structure–property relationships results in a wide range of PU applications in foams,⁸ rubbers,⁹ and coatings.¹⁰

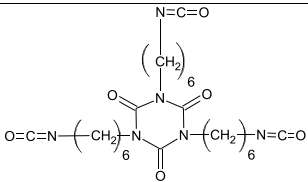
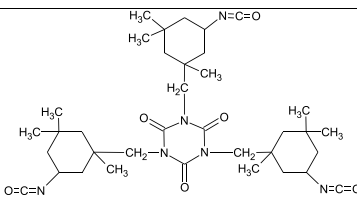
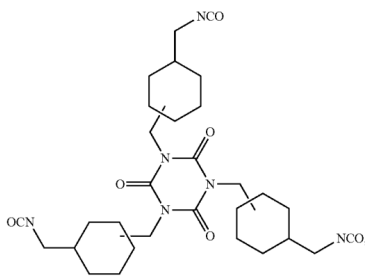
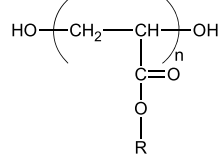
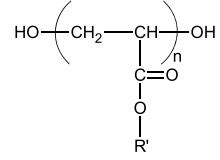
High throughput screening (HTS) is of particular interest to many applications that require rapid screening of limited quantities of material. HTS has proved to be an effective method for characterizing and optimizing new materials in applications including fuel cells,¹¹ catalysis,^{12,13} and drug delivery.¹⁴ By measuring many data points simultaneously or rapidly over a small volume or area, HTS reduces the time and cost associated with conventional single-measurement techniques. In polymer science, fabrication techniques have been developed to create polymer libraries with continuous gradient or discrete properties (e.g., annealing temperature,^{15,16} composition,¹⁷ thickness,¹⁸ etc.) to more efficiently explore the parameter space and further reduce the material, time, and cost of utilizing HTS. In conjunction with HTS, combinatorial

Received: August 5, 2019

Accepted: October 1, 2019

Published: October 1, 2019

Table 1. Structures and Properties of Monomers Used in This Study

Chemicals	Structure	Description	Solids wt. %	T_g [°C]
Desmodur N-3390 (DN)		Aliphatic polyisocyanate based on HMDI	90	-59
Desmodur Z-4470 (DZ)		Cycloaliphatic polyisocyanate based on IPDI	69.6	61
Aliphatic diisocyanate trimer (AT)		Aliphatic polyisocyanate, proprietary	70	38
Desmophen A-365 (DA)		Hydroxyl-terminated polyacrylate, proprietary	57	23
Joncryl 920 (J9)		Modified acrylic copolymer, proprietary	69.7	-5

libraries are especially useful in the early phases of material discovery when little is known about the material.^{19,20} In addition, HTS is viewed as being an important experimental counterpart to computational theory and data science in developing informatics/genomic approaches to new materials development.²¹

Polymeric surface deformation is classified as either mar or scratch damage. A mar is a mark caused by a sliding body that is too shallow to be perceived by the human eye alone, whereas a scratch is a mark that forms visible and deep grooves and usually permanent surface damage or failure.^{22,23} Scratch damage can be further classified as rough trough, cracking, delamination, and chipping and evaluated based on the size or number of damaged areas/cracks and the critical force values that demarcate transitions between damage types. During scratch damage, plastic flow and brittle fracture can each play a role. Plastic flow occurs when a yield stress is exceeded,

resulting in lateral and radial displacement of material around the indentation.²⁴ Brittle coating fractures can be classified as through thickness cracks²⁵ or interfacial failure²⁶ and are characterized by cracking, buckling, spallations, and chipping.

Despite the relative importance of HTS, most of the developments occur industrially, and very little has been published in the open literature regarding use of HTS to measure scratch damage to polymers and coatings.²⁷ Scratch tests provide a means for characterizing the resistance of polymer films and coatings to deformation under normal and shear forces applied simultaneously by an indenter. A number of scratch tests have been reported for characterizing polymer films, including both nanoscopic and microscopic methods.²² For example, a nanoindenter can be used to measure the critical forces for elastic and plastic deformation in automotive clear coatings.²⁸ Progressive loadings using a 1 mm diameter stainless steel ball give information regarding the critical forces

for the onset of coating delamination, transverse cracking, and buckling failure.²⁹ By use of the basic tools of constant and progressive load tests, new characterization methods have been developed to measure crack density and create libraries of scratches using cross-scratching techniques.²⁹

Here, we investigate a series of three-component PU films composed of mixtures of two polyisocyanates based on 1,6-hexamethylene diisocyanate (HMDI), isophorone diisocyanate (IPDI), and two polyols based on hydroxyl-terminated polyacrylate and a modified acrylic copolymer. The PU components used in this study were selected because of the broad range of glass transition temperatures (T_g). Because the ability to adjust the bulk mechanical properties and the scratch resistance is a significant concern in the application of polyurethane clear coatings, we seek to identify a subset of systems where one can tune mechanical and mar/scratch properties based on knowledge of the thermal properties of the precursors, composition, and curing conditions. The present study compares high throughput mechanical tensile and scratch resistance properties for a large library of tricomponent PUs that explores both composition and processing conditions. A library of films was fabricated to enable identification of effects of composition (3 levels), chemistry (7 systems), and curing conditions (3 conditions) using semiautomated ATR-FTIR, high throughput mechanical (HTMECH),^{17,30} and high throughput scratch (HTScratch) characterization.

EXPERIMENTAL SECTION

Materials. The three isocyanates—Desmodur N-3390 (90 wt % in *n*-butyl acetate, Bayer Material Science), Desmodur Z-4470 (70 wt % in *n*-butyl acetate, Bayer Material Science), and an aliphatic diisocyanate (ADI) trimer (70 wt % in *n*-butyl acetate, Dow Chemical)—and the two polyols—Desmophen A-365 (65 wt % in *n*-butyl acetate and xylene, Bayer Material Science) and Joncryl 920 (80 wt % in *n*-butyl acetate and methyl *n*-amyl ketone, BASF)—were diluted with butyl acetate (BDH Chemicals) to match their viscosities (~1000 cP). Their chemical structures and relevant properties are given in Table 1.

Substrate Preparation. Untreated glass substrates were cleaned with a piranha solution of 75 vol % sulfuric acid (97%, BDH Chemicals Ltd.) and 25 vol % hydrogen peroxide (30 wt %, BDH Chemicals Ltd.) at 80 °C for 1 h. The cleaned glass substrates were then immersed for 1 h in a 0.1 vol % octadecyltrichlorosilane (OTS 95%, Acros Organics) solution in toluene, previously aged for 1 h, and subsequently washed with toluene, ethanol, and water.

PU Film Fabrication. A series of discrete composition PU films composed of polyisocyanates of Desmodur-N-3390 (DN), Desmodur Z-4470 (DZ), and ADI Trimer (AT) blended with polyols of Desmophen A-365 (DA) and Joncryl 920 (J9) were fabricated with varying curing conditions to study the relationships between curing conditions and mechanical properties. In all blends a constant 1:1 mole ratio of NCO:OH groups was maintained to minimize the amount of unreacted NCO and OH groups remaining after the formation of urethane linkages. The effect of PU composition on mechanical properties was studied either by varying the OH mole ratio between two polyols in blends of one polyisocyanate and two polyols (NCO:OH₁:OH₂) or by varying the NCO mole ratio between two polyisocyanates in blends of one polyol with two polyisocyanates (OH:NCO₁:NCO₂). The three mole ratios of reacting groups studied in every PU blend were 0.5:0.1:0.4, 0.5:0.25:0.25, and 0.5:0.4:0.1.

Quaternary mixtures containing solvent and either two polyisocyanates and one polyol or one polyisocyanate and two polyols were infused into a 300 μ L gradient mixing chamber at a total flow rate of 0.3 mL/min by using three computer-controlled NE-500 syringe pumps (New Era Pump Systems, Inc.). The custom-built device utilized to carry out mixing and deposit coatings is described in detail elsewhere.³¹ The PU components were fed at constant mole

flow rates for constant composition films. The tubular mixing chamber, constructed by using a Swagelok union (SS-400-6) as the body, was equipped with an impeller (Dealt, Inc. Model 196). The impeller shaft, sealed by using Teflon tubing to prevent liquid leakage while allowing rotation, was coupled to a motor that operated at 1500 rpm. Three Teflon inlet tubes (1/8 in. outside diameter) were fitted to the base, and one Teflon outlet tube (1/8 in. outside diameter) was fitted to the chamber head. In all cases the Reynolds number in the tubing was well below the laminar flow limits ($N_E \ll 2100$) for the blend products, ensuring that no turbulent mixing occurred after exiting the mixer. The outlet tube connects to a vertically mounted microchannel coating blade, with an internal volume of 75 μ L designed to provide equal residence times for the solution in each of the 16 channels, which deposits the constant composition blend or continuous composition gradient onto a suitable substrate supported on a motion control stage (Parker Daedal) to form the desired film. The thickness of the film can be controlled by adjusting either the blade height or the speed of the motion control stage. After casting, films prepared by using *n*-butyl acetate as the solvent were dried according to the three curing conditions listed in Table 2.

Table 2. Curing Conditions of PU Films Fabricated in This Study

label	curing conditions
C1	60 °C for 1 day followed by 120 °C for 3 days
C2	120 °C for 30 min followed by room temperature (23 °C) for 3 days
C3	room temperature (23 °C) for 7 days

Room temperature curing was not performed at atmospheric pressure, rather than under vacuum, to prevent rapid solvent evaporation and bubble formation. PU films cured in a vacuum oven were cast onto OTS-treated glass substrates, with a static water contact angle of $95.7 \pm 0.7^\circ$, to facilitate easy removal of the films for characterization. PU films cured at room temperature were cast onto aluminum substrates with a static water contact angle of $64.7 \pm 1.4^\circ$ to prevent dewetting of the film during drying. Film thicknesses were typically between 150 and 250 μ m. A total of 57 conditions were explored in the library of films produced herein, consisting of three compositions and three curing conditions prepared for up to seven combinations of precursors. In addition, all films were prepared in triplicate, and characterization was performed in triplicate for each condition, leading to a total of $3 \times 57 = 171$ independent samples.

Characterization. Static water contact angles were measured on the different substrates by using an AST Products video contact angle 2500 XE system. A 1 μ L water drop was dispensed onto the surface of the substrate. The contact angles between the substrate and the tangent line to the left and right side of the water drop were fit for five measurements.

The discrete composition PU films and the gradient library casted on glass or aluminum substrate were characterized by attenuated total reflectance infrared (ATR-FTIR) spectroscopy. ATR-FTIR spectroscopy measurements were performed using a Broker Vertex 80v FTIR spectrometer coupled to a Hyperion 2000 IR microscope under a 20 \times magnification ATR objective with a germanium crystal. The ATR-FTIR signals averaged over 64 scans were collected in the mid-IR range, 4000–400 cm^{-1} with a resolution of 4 cm^{-1} , by using a Kerr beam splitter. The FTIR software was used to baseline correct each spectrum and correct the wavelength-dependent variation in penetration depths of the IR radiation before further analysis.

Mechanical characterization of PU films was performed on a custom-built HTMECH apparatus, which has been described in detail in prior literature.^{17,30} The PU films were mounted in between two stainless steel plates, containing 10×10 grids of 3 mm diameter holes, attached to a linear motor. The holder containing the film was then moved at a rate of 1 mm s^{-1} toward a 33.7 mm long shaft possessing a 1 mm hemispherical tip connected to a high-sensitivity load cell. The film is indented by the shaft, and a force versus time profile is generated as the film is biaxially deformed until it fractures.

The force versus time data are then demised and analyzed with a custom-developed algorithm to extract mechanical properties of the films (e.g., toughness, strain at break, ultimate tensile strength, normalized maximum force, and elastic modulus). A minimum of 20 stress–strain profiles were measured on each PU film.

HTScratch characterization was performed by modifying the HTMECH apparatus. A schematic of the instrument is shown in Figure 1a. PU films attached to a stainless steel plate were mounted

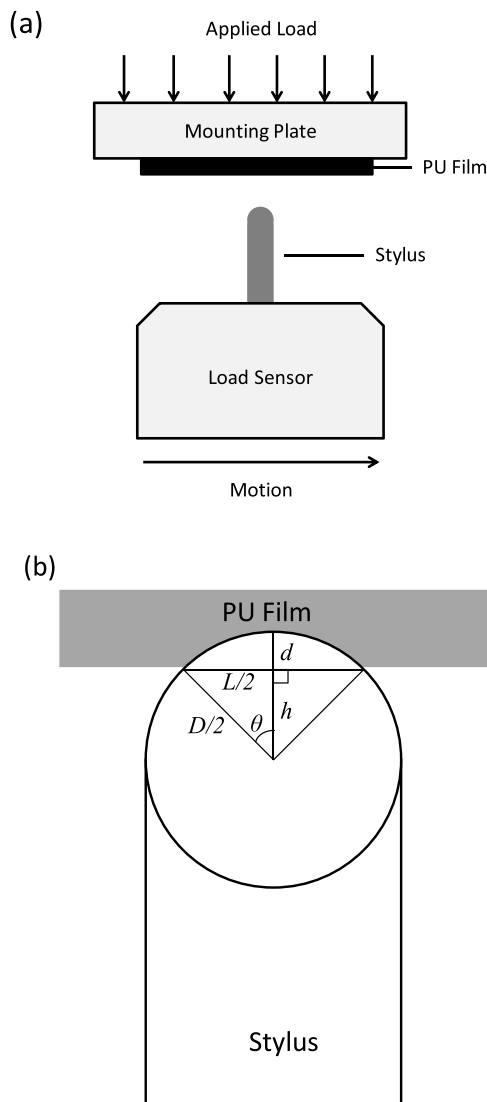


Figure 1. (a) Cross-sectional schematic of the HTScratch apparatus, in which the load sensor can be moved in two axes in a plane normal to this page, to select locations on a film library. The films are attached to an upper mounting plate that is connected to a linear motor with closed-loop control of applied load in the vertical direction. (b) Geometric relationships used to determine the scratch depth of the HTScratch stainless steel stylus. The scratch depth (d) is calculated from the scratch width (L) and the stylus diameter (D).

on the underside of a mounting plate attached to the linear motor. The film was then contacted with a BYK Gardener stainless steel stylus with a 12.7 mm long shaft and a 1.59 mm diameter spherical tip connected to the high-sensitivity load cell. The linear motor applied constant normal forces of 4, 8, 16, 24, and 36 N to the film, and the stylus/load cell assembly moved 10 mm across the film to test its mar resistance. Polymer films subjected to deformation by a spherical ball under defined loads can be inspected optically by using an automated microscope to provide information about the critical load for failure

and the mar resistance. An Olympus BX51 upright microscope was used to inspect the HTScratch deformations under 4 \times magnification. Three scratches were made for each condition in the film library. Uncertainties in all data are measured with a 95% confidence interval. The widths of HTScratch deformations are measured and related to scratch depths, shown in Figure 1b. Simple geometric relationships are used to determine the scratch depths of the HTScratch deformations: $\theta = \sin^{-1}(L/D)$, $h = L/(2 \tan(\theta))$, and $d = D/(2 - h)$. Here, h and θ are characteristics of the right triangle, L is the width of the deformation, D is the diameter of the stainless steel stylus, and d is the scratch depth. Assays were performed on each sample in the 171 member library: FTIR-ATR (3 replicates), HTMECH (20 replicates), and HTScratch (3 replicates with 5 loadings, including optical inspection), as discussed below. Including replicates and multiple loading conditions discussed above for each of these assays, the total number of independent characterizations performed was 2166. For 18 selected systems, additional differential scanning calorimetry (DSC) (Q200, TA Instruments) was performed to determine the glass transition temperature (T_g) of polyurethane films. Small pieces of cut films, 9–10 mg in weight, were loaded in aluminum pans and sealed with lids, and then the samples were heated from -50 to 250 $^{\circ}\text{C}$ at a rate of 10 $^{\circ}\text{C min}^{-1}$ under a nitrogen gas flow.

The HTMECH and HT-SCRATCH measurements were performed in a high throughput serial collection mode, with manual reloading of samples. Approximately 20 HTMECH stress–strain replicates can be collected per loaded sample in 3 min, including sample loading time. For HT-SCRATCH characterization a complete load series for one sample can be collected in 5 min, including sample reloading. The entire set of HTMECH data for 57 samples required 170 min and for HT-SCRATCH required 285 min. The FTIR and optical microscopy were assisted by automated sample positioning stages used to select the position on the sample. However, the sample had to be manually placed on the instrument following each measurement. FTIR and OM were relatively rapid semiautomated measurements, requiring 2–5 min for each sample. With the exception of TGA, which was run conventionally on only 18 samples, the elapsed time for data collection for the entire set was about 14 h.

RESULTS AND DISCUSSION

The J9:DN:DZ and DA:DN:DZ systems, which combine a single polyol (J9 or DA) with a blend of the DN and DZ isocyanates, showed the most sensitive variation in mechanical and scratch properties, so they are discussed in the most detail in this study, although results are presented for all 57 sample types and conditions represented in the libraries. FTIR-ATR spectra are shown in Figure 2 (NCO vibration range) and Figure S1 (Supporting Information, carbonyl vibration range) for the J9:DN:DZ and DA:DN:DZ blends cured at C1, C2, and C3 (Table 2) conditions. The presence of a PU structure is verified by the carbonyl ($\text{C}=\text{O}$) stretching vibration of the isocyanurate ring at 1695 cm^{-1} and free urethane $\text{C}=\text{O}$ stretching at 1723 cm^{-1} in Figure S1.³² The extent of curing is monitored by the intensity of the NCO group vibration at 2275 cm^{-1} in Figure 2.³³ The intensity of this peak indicates the decreasing presence of unreacted NCO groups as the curing temperature increases. The extent of curing was always complete for condition C1 (which is the only condition that employed elevated temperature for more than 30 min). However, some amount of uncured NCO remained for C2 and C3, both of which consisted of a 7 day room temperature cure, with C2 showing a more complete cure than C3 due to the initial 30 min duration of 120 $^{\circ}\text{C}$ curing in C2. The extent of cure was nearly always higher with higher content of the low- T_g DN isocyanate versus the high- T_g DZ isocyanate, suggesting a role of isocyanate mobility in the rate or extent of

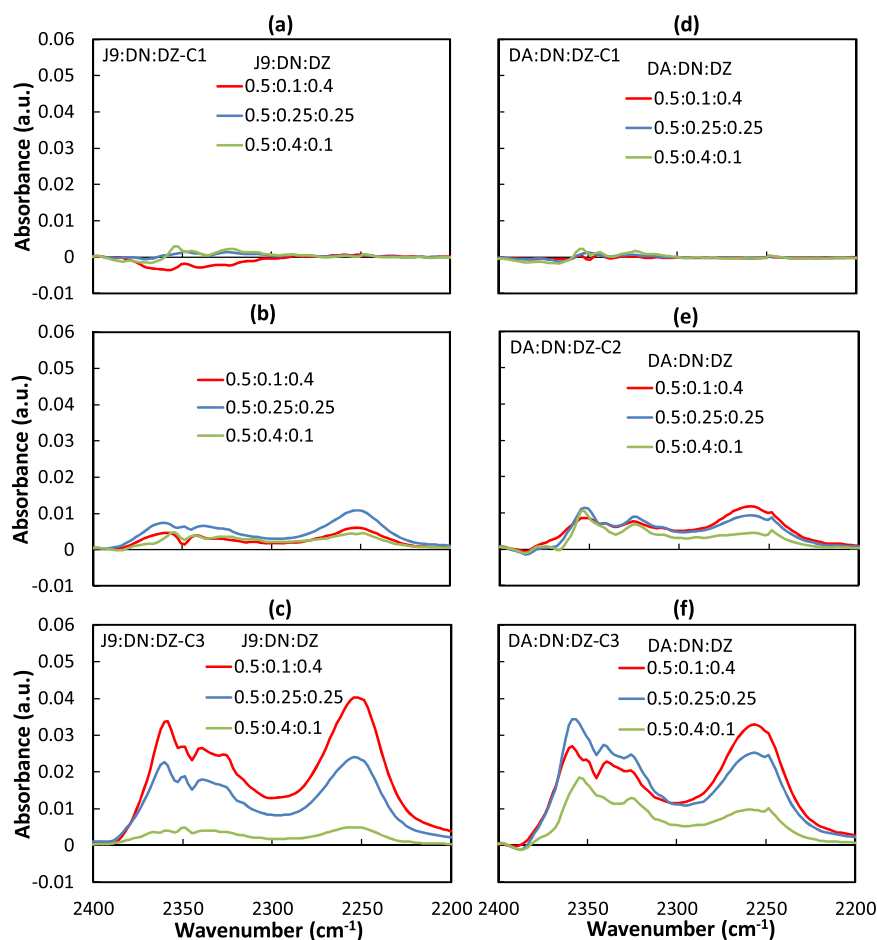


Figure 2. ATR-FTIR spectra of (a–c) J9:DN:DZ and (d–f) DA:DN:DZ PU formulations with mole ratios of (red) 0.5:0.1:0.4, (blue) 0.5:0.25:0.25, and (green) 0.5:0.4:0.1 in the NCO vibration region cured at C1 (a, d), C2 (b, e), and C3 (c, f).

cure. The NCO groups on the polyisocyanates (DN and DZ) are capable of reacting with water to form a urea linkage characterized by a free urea carbonyl ($\text{C}=\text{O}$) vibration at 1691 cm^{-1} and hydrogen-bonded carbonyl ($\text{C}=\text{O}$) vibrations at 1666 and 1643 cm^{-1} .³⁴ Small increases in these absorbances in Figure S1 at C2 and C3 may indicate small quantities of urea linkages have formed.

Figure 3 presents HTMECH results of [polyol:isocyanate 1:isocyanate 2] blends containing J9 and DA polyols prepared at condition C1, while the full set of HTMECH results at other curing conditions C2 and C3 are shown in Figures S2 and S3, respectively. From a cursory examination of the results of the entire set, one can see that significant property tunability emerges for only a small subset of the compositions and curing conditions explored. Only the J9:DN:DZ, DA:DN:DZ, J9:DN:AT, and DA:DN:AT systems demonstrated any appreciable trends where differences in toughness, strain at break, ultimate tensile strength, elastic modulus, and scratch resistance can be attributed to variations in composition and curing condition. All of these are systems containing a single polyol reacted with a blend of isocyanates and where the T_g 's of the two isocyanates are quite different; i.e., one is below room temperature (DN), and the other is above room temperature (DZ or AT) (Table 1). In fact, the behavior of the systems containing the high- T_g isocyanate DZ is quite similar to that containing AT, which is not surprising given that both are derived from cycloaliphatic triisocyanates. Therefore,

the remainder of the in-depth analysis will focus therefore on the J9:DN:DZ and DA:DN:DZ systems. A few additional remarks are noteworthy before proceeding. (i) The most tunability (highest sensitivity to composition and curing condition) appears in samples cured at either C1 or C3, which represent the extremes of curing, where C1 is a relatively short cure with high T and C3 is a long-term room T cure. (ii) The sample that contains blended polyols does not show any trend, even though the two polyol T_g 's are fairly different at $-5\text{ }^\circ\text{C}$ (J9) and $23\text{ }^\circ\text{C}$ (DA). (iii) The samples that vary isocyanate ratio with DZ:AT show very little tunability. This is perhaps unsurprising because their monomer T_g values are relatively close (38 and $61\text{ }^\circ\text{C}$), both are above room T , and they are of similar cycloaliphatic chemistry.

Table 3 shows T_g values of films following curing at conditions C1, C2, or C3, for J9:DN:DZ and DA:DN:DZ samples. Within each sample set, the T_g decreases as the ratio of DN:DZ increases, in agreement with expectations based on the T_g values of the monomers DN ($T_g = -59\text{ }^\circ\text{C}$) and DZ ($T_g = 61\text{ }^\circ\text{C}$), as shown in Table 1. Generally, the T_g of the DA-type polyol samples is higher than the T_g of the samples containing J9-type polyol, which is also in agreement with the order of T_g values of those polyols, shown in Table 1. J9 has a monomer T_g of $-5\text{ }^\circ\text{C}$, and DA has a T_g of $23\text{ }^\circ\text{C}$. However, the J9:DN:DZ system does not follow the same trend as the DA-containing polyol system regarding response to curing conditions. In the DA-containing system, the T_g monotonically

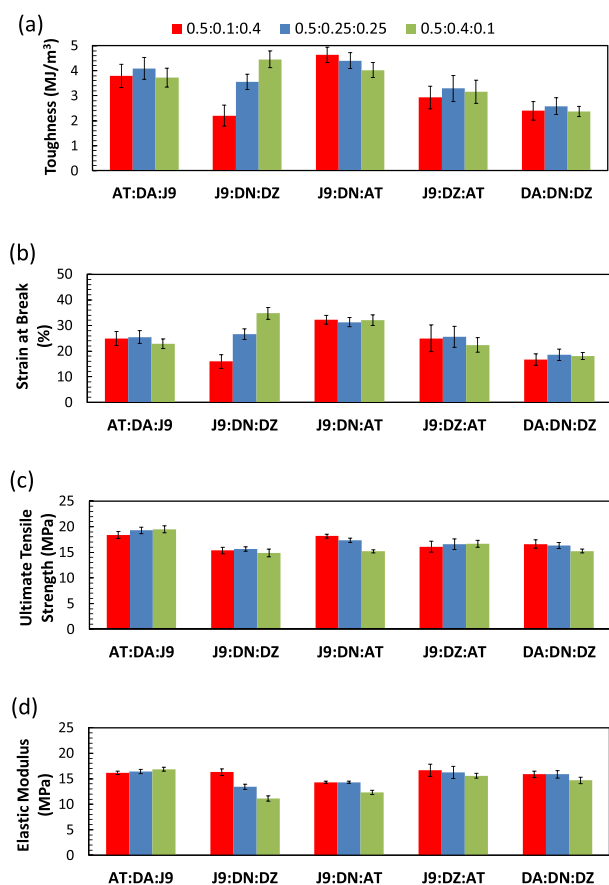


Figure 3. HTMECH analysis of (a) toughness, (b) strain at break, (c) ultimate tensile strength, and (d) elastic modulus in PU formulations with mole ratios of (red) 0.5:0.1:0.4, (blue) 0.5:0.25:0.25, and (green) 0.5:0.4:0.1 at C1.

Table 3. T_g Determined by DSC for Selected PU Blends at Three Curing Conditions

PU composition	C1	T_g (°C)		
		C2	C3	
J9:DN:DZ				
0.5:0.1:0.4	88	79	126	
0.5:0.25:0.25	68	70	60	
0.5:0.4:0.1	45	51	42	
DA:DN:DZ				
0.5:0.1:0.4	100	99	92	
0.5:0.25:0.25	83	82	74	
0.5:0.4:0.1	62	61	62	

decreases as the curing condition becomes longer and lower T (C1 to C2 to C3). In the J9-containing systems, the T_g does not monotonically decrease from C1 to C2 to C3 at a given composition. In fact, one of the surprising points is that the system J9:DN:DZ with composition 0.5:0.1:0.4 has the highest T_g by a significant margin (126 °C) when cured at conditions C3, which is a 7 day room temperature cure.

Associated with this high T_g for J9:DN:DZ 0.5:0.1:0.4 is a low strain at break and high modulus and UTS (Table S1 and Figure 3) compared to the other compositions at the same condition C3. In addition, this sample had unusually poor scratch resistance (Figure S5), with high value of scratch depth compared to C1 or C2, at the same composition, and was

brittle, showing failure at applied loads above 16 N. One caveat of the T_g measurements is that they were performed several weeks following the sample curing protocols. During this time period, the sample that was not completely cured likely continued to slowly cure at room T . We propose that the high T_g for J9 at C3 results from the network structure that emerges due to slow curing at low T , interfering side reactions with water vapor become more likely. These form urea linkages rather than urethane, and Figure S1c shows evidence of urea formation in this sample, with absorbances near 1650 cm^{-1} typical of urea carbonyls. In addition, the self-reaction of excess isocyanate with a urethane to form an allophanate may proceed slowly over weeks at room temperature and results in additional cross-linking. Finally, during a slow cure over many days, there is time for diffusion of the un-cross-linked components into phase-separated structures driven by intermolecular interactions, such as urethane or urea hydrogen bonding.

Figure 2d (FTIR) indicates that the J9:DN:DZ 0.5:0.1:0.4 system had the highest quantity of uncured NCO group at the time of the FTIR measurement (24 h following curing). Interestingly, the DA:DN:DZ 0.5:0.1:0.4 sample (Figure 2e) also had high uncured content for C3. However, DA has a higher T_g than J9 (23 versus 9 °C), and as a result the J9 sample is expected to allow more rearrangement and diffusion during the course of a slowly evolving cure reaction. The FTIR also illustrates the important role of the reactivity of the isocyanate component, which changes significantly as the ratio of DN:DZ changes. For example, for J9:DN:DZ containing more DN (0.5:0.4:0.1), the extent of curing at C3 is much higher (Figure 2c) than for the sample containing the most DZ (0.5:0.1:0.4), which indicates the differential reactivities of DN (faster) versus DZ at room T .

Numerical values of mechanical properties from Figure 3 are shown in Table S1 for the two systems that showed the most variation controllable by composition: J9:DN:DZ and DA:DN:DZ. A single factor analysis of variance was performed on these two systems (containing J9 or DA polyol) to identify situations in which variation was at least at the 5% significance level. The mechanical properties of each blend were compared in two groups: group 1 held constant mole ratios while varying curing conditions and group 2 held constant curing condition while varying mole ratios. Of the 48 possible groupings, only six groups did not show significantly different means, indicated by asterisks in Table S1. Examining the effects from group 1, toughness, strain at break, ultimate tensile strength, and elastic modulus did not exhibit any trends with curing condition. Examining the compositional effects from group 2, however, the ultimate tensile strength and elastic modulus decreased monotonically with increasing DN:DZ molar ratio in blends containing these two isocyanates. In contrast, toughness and strain at break increased monotonically as the fraction of lower T_g DN increases.

Toughness, strain at break, ultimate tensile strength, and elastic modulus data for the PU blends of J9:DN:DZ and DA:DN:DZ are plotted versus film T_g in Figures 4a, 4b, 4c, and 4d, respectively. Examining the effects of T_g blends rich in the high- T_g DZ, possess lower toughness and strain at break than blends rich in the low- T_g DN. At room temperature (C3), Figures 2c and 2f show that J9:DN:DZ and DA:DN:DZ PU blends rich in DN cure to a greater extent than blends rich in DZ. It is expected that toughness and strain at break would

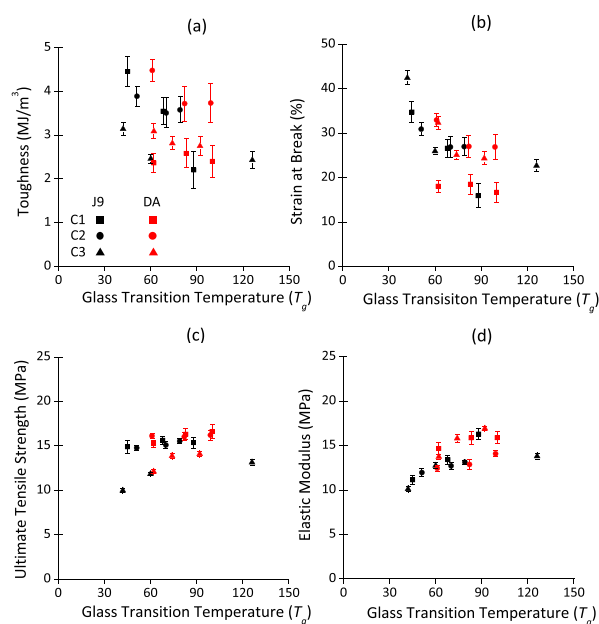


Figure 4. HTMECH analysis of (a) toughness, (b) strain at break, (c) ultimate tensile strength, and (d) elastic modulus in PU formulations of (black) J9:DN:DZ and (red) DA:DN:DZ cured at C1, C2, and C3 denoted by squares, circles, and triangles, respectively.

decrease as the T_g of the blend increases, shown in Figures 4a and 4b, and it is likewise expected that elastic modulus, Figure 4d, increases with T_g . Because the strain rate is held constant and the films are all indented until failure, an increase in strain at break corresponds to a decrease in elastic modulus. The ultimate tensile strength in Figure 4c does not show a strong dependence on T_g . Only PU blends cured at C1 are completely cured (Figures 3d and 3j), while systems cured at C2 and C3 have some amount of unreacted NCO groups present, from Figure 2. Blends cured at the intermediate C2 do not follow the expected trend with T_g . Overall, it appears that DN-rich blends are softer (i.e., higher strain at break) and more ductile (i.e., higher toughness) than DZ-rich blends but that this trend is expressed most profoundly in the fully cured systems.

The effects of polyol chemistry can be assessed in comparing the J9:DN:DZ and DA:DN:DZ systems. A decrease in toughness and strain at break of J9:DN:DZ with DN composition in Figures 5a and 5b, respectively, correlates well with the increase in blended polyisocyanate T_g as DZ fraction increases. However, the DA:DN:DZ system shows no such correlation. Additionally, an increase in elastic modulus of the J9:DN:DZ system in Figure 4d corresponds to an increase in polyisocyanate T_g , but the DA:DN:DZ system does not show this correlation. The ultimate tensile strength, shown in Figure 4c, does not show a strong dependence on polyol chemistry. The T_g of pure J9 and DA is -5 and 23 °C (near room temperature where mechanical tests are performed), respectively. Only the formulations containing the softer polyol, J9, show any dependence of mechanical properties on the ratio of soft-to-hard isocyanate, DN:DZ. We tentatively conclude that sensitive dependence of mechanical properties on T_g of the polyisocyanates requires a relatively soft polyol with T_g below room temperature.

Representative optical microscope images of scratch images resulting from HTScratch deformations are displayed in Figure 5 and allow for observing the width of scratches and presence

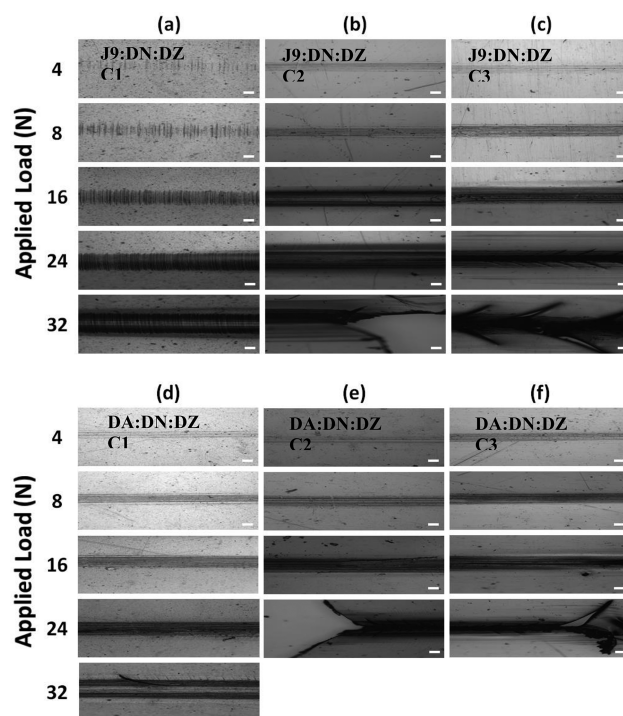


Figure 5. Representative scratch images at various applied loads of (a–c) J9:DN:DZ PU and (d–f) DA:DN:DZ formulations with a mole ratio of 0.5:0.25:0.25 cured at C1 (a, d), C2 (b, e), and C3 (c, f) (scale bar indicates $140 \mu\text{m}$).

of film failure, characterized by cracking and fracturing at high applied loads. The widths of scratch deformations are measured from the images, and scratch depths are estimated from simple geometric relationships, as described in the Experimental Section. Complete HTScratch results of the PU formulations of AT:DA:J9, J9:DN:DZ, J9:DN:AT, J9:DZ:AT, DA:DN:DZ, DA:DN:AT, DA:DZ:AT, and DN:DA:J9 with compositions of 0.5:0.1:0.4, 0.5:0.25:0.25, and 0.5:0.4:0.1 cured at C1, C2, and C3 are shown in Figures S4, S5, and S6, respectively. In general, scratch depth increased linearly with applied load. The experimental error associated with HTScratch measurements, shown in Figure S7, is typically within 10% of the mean value.

The J9:DN:DZ and DA:DN:DZ scratch data offer further support for the relationships observed from HTMECH analysis. From the images of the 0.5:0.25:0.25 J9:DN:DZ and DA:DN:DZ systems in Figure 5, it is apparent that curing condition has a significant effect on the deformation resistance. The more fully cured systems showed better resistance to scratching (narrower deformations) and better resistance to failure than the less fully cured systems. Figure 6 provides the maximum scratch depths observed at any loading for the J9:DN:DZ and DA:DN:DZ systems cured at C1, C2, and C3 for all three compositions examined. Of the 18 total PU blends, only four films do not experience failure at any applied load (indicated by the absence of crosshatching in Figures 6a and 6b). In general, the J9-containing systems showed larger scratch depths but resisted cracking and failure to higher loadings than DA-containing systems when compared at the same curing condition. The complete data sets in Figures S4–S6 also reveal this detail. This is sensible given the lower T_g (in general) of the J9 monomer itself than the DA monomer. Generally the J9 systems that cured completely (C1) in short

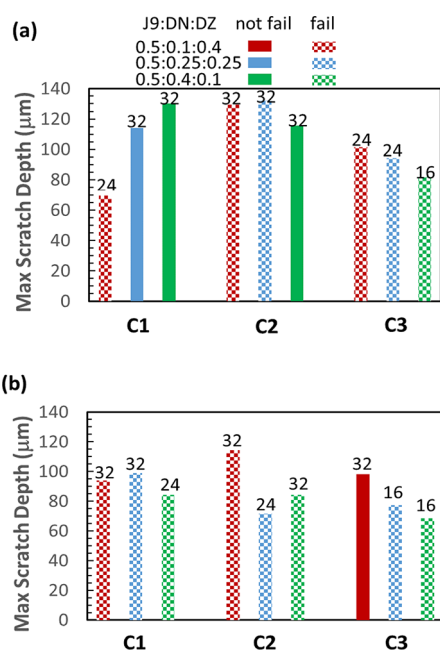


Figure 6. Maximum scratch depths of (a) J9:DN:DZ PU and (b) DA:DN:DZ formulations with mole ratios of (red) 0.5:0.1:0.4, (blue) 0.5:0.25:0.25, and (green) 0.5:0.4:0.1 cured at condition 1 (C1), condition 2 (C2), and condition 3 (C3). Crosshatching indicates failure during the scratch measurement at the maximum applied load.

time resist failure to higher loadings than the DA systems cured at C1. This finding is consistent with the toughness values in Figure 3a, where toughness increases dramatically with the DN:DZ ratio for the J9 system, but all toughnesses for the DA system were about the same as the least tough J9 system. Thus, the J9:DN:DZ systems displayed an unusual ability to withstand damage without failing compared to the DA:DN:DZ systems, and the extent of deformation (scratch depth) could be rationally adjusted over a wide range in the J9 system. When all compositions are examined, it is apparent that blends cured at room T for 7 days (C3) failed at the lowest applied load. These blends, especially the DA:DN:DZ samples, had correspondingly high elastic moduli compared to others (Figure 4) and were quite brittle, as discussed in detail previously with the T_g data in Table 3.

Encoded within the data in Figures 5 and 6 are dependencies on T_g . The effects of T_g on the maximum scratch depth are shown in Figure 7a–c. The J9:DN:DZ system showed that the maximum scratch depth decreased with increasing T_g under curing condition C1 (fully cured), an intuitive result. However, this system showed the opposite trend under conditions C2 and C3. The J9:DN:DZ system follows the expectation that fully cured films rich in low- T_g DN resist fractures at higher loads, but are more susceptible to scratching, than fully cured high- T_g DZ-rich blends. Additionally, completely cured (C1) J9:DN:DZ PU blends in Figure 7a that are rich in DN are softer and more ductile than DZ-rich blends. These trends in the scratch resistance and cracking with film T_g composition, and curing are similar to those observed in the mechanical data (Figure 3 and Table S1). Notably the J9:DN:DZ system is identified as the one that responds most sensitively to tuning in both mechanical and scratch property analysis. This system is characterized by a soft polyol that is reacted with a blend of soft and hard triisocyanates, where the tunability in bulk mechanical properties and scratch resistance can be achieved

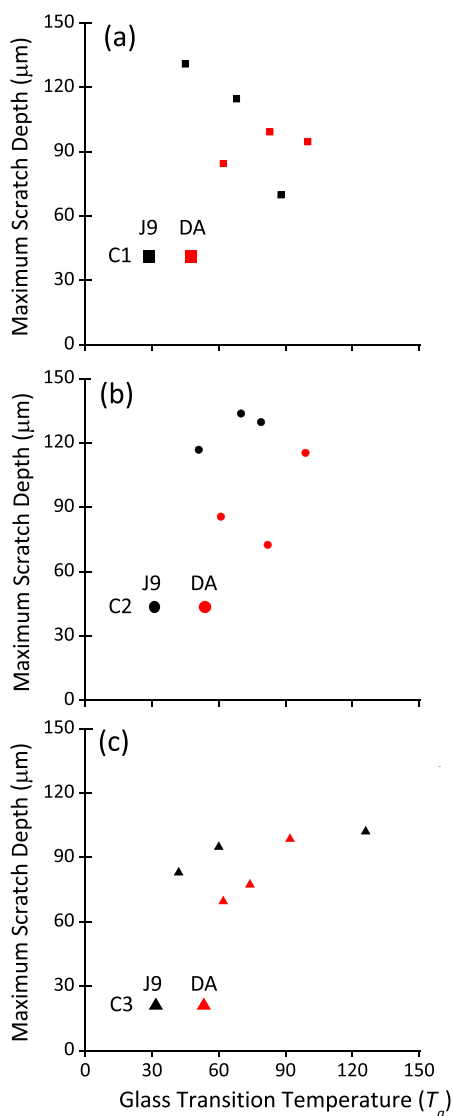


Figure 7. Maximum scratch depth under curing conditions (a) C1, (b) C2, and (c) C3 in PU formulations of (black) J9:DN:DZ and (red) DA:DN:DZ.

by adjusting the ratio of soft and hard isocyanates. What we also observe is that the curing condition is significant in determining which composition trend is observed. In general, the DA:DN:DZ system showed a counterintuitive increase in maximum scratch depth with increasing T_g , with only one data point in exception (0.5:0.25:0.25 in Figure 7b). As noted above, the J9-containing systems also display this counterintuitive behavior when not fully cured. However, it must be kept in mind that these samples usually fail at lower loadings than others, so that the maximum scratch depth reported is observed at a lower loading. Figure 7 shows the maximum observed scratch depth at any loading, whether the sample failed or not at that maximum point. It is a summary showing maximum observed depth and sample failure loading simultaneously. For the J9 system, the reversal of the trend between C1 (scratch depth decreases with T_g) versus C3 (scratch depth increases with T_g) is associated with the onset of failure (cracking) that occurs at lower loadings in sample C3 (see Figures S4 and S6 for the scratch depth at all loadings).

All samples at C3 failed at either 16 or 24 N, whereas two of the three samples at C1 did not fail at all even at the highest loading of 32 N. There is an obvious embrittlement associated with the J9:DN:DZ system when it is cured slowly over a long period (C3) compared to short, fast cure (C1) at high T . The possible reasons for the formation of a more brittle, higher T_g network structure over long-term cure were discussed in the section on T_g associated with Table 3. For sample set DA:DN:DZ, very often there is either little trend or the scratch depth increases with softer DN content as would be expected, when examined for lower loadings prior to failure, e.g., 8 or 16 N. These are seen as Figures S4e, S5e, and S6e.

CONCLUSIONS

In summary, HTS of mechanical properties in PU films composed of polyisocyanates of DN, DZ, and AT blended with polyols of DA and J9 was accomplished with FTIR-ATR, HTMECH, and HTScratch characterization. In particular, the effect of blending polyisocyanates (or polyols) in ternary mixtures was explored at three curing conditions. An important question relevant to applications in coatings that use ternary blends is the extent to which mechanical and scratch resistance properties can be tuned rationally. Many of the combinations of blended polyol or blended isocyanate PUs showed little compositional or curing effect on mechanical properties and scratch resistance. However, a class of systems where mechanical and scratch resistance properties could be tuned via composition and curing were identified. These were all systems that contained a single polyol combined with a blend of two triisocyanates, where the two isocyanates had a glass transition temperature below and above room temperature. Specifically, these corresponded to the J9:DN:DZ, DA:DN:DZ, J9:DN:AT, and DA:DN:AT samples. In these systems, the tunable effects of isocyanate or polyol T_g on mechanical properties (scratch resistance, modulus, and strain at break) were most evident only for the highest T curing condition that produced the most fully cured films. These effects were also most evident in the system containing a soft polyol, J9, with T_g below room T . In general, for the fully cured systems the trends in scratch resistance followed trends observed in bulk mechanical properties (HTMECH). These properties generally followed the trend that DN-rich blends were softer materials (i.e., lower modulus and higher maximum scratch depth as the composition of DN increased) but more ductile (i.e., higher strain at break as the composition of DN increased) when compared to DZ-rich blends. Interestingly, these trends were sometimes absent, or even reversed, when the systems were cured less completely, which indicates an important advantage of applying a high throughput methodology to screen large numbers of combinations of curing and compositional variables.

ASSOCIATED CONTENT

Supporting Information

The Supporting Information is available free of charge on the ACS Publications website at DOI: 10.1021/acsapm.9b00726.

FTIR-ATR spectra in the carbonyl region; complete HTMECH and HT-SCRATCH data at all curing conditions for all compositions explored; detailed plot of scratch depth versus loading force for determining experimental uncertainty of HT-SCRATCH (PDF)

AUTHOR INFORMATION

Corresponding Author

*E-mail Carson.Meredith@chbe.gatech.edu.

ORCID

J. Carson Meredith: 0000-0003-2519-5003

Notes

The authors declare no competing financial interest.

ACKNOWLEDGMENTS

The Dow Chemical Company is gratefully acknowledged for financial support of this research.

REFERENCES

- (1) Akindoyo, J. O.; Beg, M. D. H.; Ghazali, S.; Islam, M. R.; Jeyaratnam, N.; Yuvaraj, A. R. Polyurethane types, synthesis and applications – a review. *RSC Adv.* **2016**, *6*, 114453.
- (2) Davies, P.; Evrard, G. Accelerated ageing of polyurethanes for marine applications. *Polym. Degrad. Stab.* **2007**, *92* (8), 1455–1464.
- (3) Simon, P.; Fratricova, M.; Schwarzer, P.; Wilde, H. W. Evaluation of the residual stability of polyurethane automotive coatings by DSC - Equivalence of Xenotest and desert weathering tests and the synergism of stabilizers. *J. Therm. Anal. Calorim.* **2006**, *84* (3), 679–692.
- (4) Temtchenko, T.; Turri, S.; Novelli, S.; Delucchi, M. New developments in perfluoropolyether resins technology: high solid and durable polyurethanes for heavy duty and clear OEM coatings. *Prog. Org. Coat.* **2001**, *43* (1–3), 75–84.
- (5) Yang, X. F.; Li, J.; Croll, S. G.; Tallman, D. E.; Bierwagen, G. P. Degradation of low gloss polyurethane aircraft coatings under UV and prohesion alternating exposures. *Polym. Degrad. Stab.* **2003**, *80* (1), 51–58.
- (6) Bruins, P. F. *Polyurethane Technology*; Interscience Publishers: New York, 1969.
- (7) Doyle, E. N. *The Development and Use of Polyurethane Products*; McGraw-Hill: New York, 1971.
- (8) Guo, A.; Javni, I.; Petrovic, Z. Rigid polyurethane foams based on soybean oil. *J. Appl. Polym. Sci.* **2000**, *77* (2), 467–473.
- (9) Doman, D. A.; Cronin, D. S.; Salisbury, C. P. Characterization of polyurethane rubber at high deformation rates. *Exp. Mech.* **2006**, *46* (3), 367–376.
- (10) Yang, X. F.; Tallman, D. E.; Bierwagen, G. P.; Croll, S. G.; Rohlik, S. Blistering and degradation of polyurethane coatings under different accelerated weathering tests. *Polym. Degrad. Stab.* **2002**, *77* (1), 103–109.
- (11) Zapata, P.; Basak, P.; Meredith, J. C. High-throughput screening of ionic conductivity in polymer membranes. *Electrochim. Acta* **2009**, *54* (15), 3899–3909.
- (12) de Bellefon, C.; Tanchoux, N.; Caravieilh, S.; Grenouillet, P.; Hessel, V. Microreactors for dynamic, high throughput screening of fluid/liquid molecular catalysis. *Angew. Chem., Int. Ed.* **2000**, *39* (19), 3442.
- (13) Matsushita, M.; Yoshida, K.; Yamamoto, N.; Wirsching, P.; Lerner, R. A.; Janda, K. D. High-throughput screening by using a blue-fluorescent antibody sensor. *Angew. Chem., Int. Ed.* **2003**, *42* (48), 5984–5987.
- (14) Kansy, M.; Senner, F.; Gubernator, K. Physicochemical high throughput screening: Parallel artificial membrane permeation assay in the description of passive absorption processes. *J. Med. Chem.* **1998**, *41* (7), 1007–1010.
- (15) Meredith, J. C.; Karim, A.; Amis, E. J. High-throughput measurement of polymer blend phase behavior. *Macromolecules* **2000**, *33*, 5760–5762.
- (16) Meredith, J. C.; Smith, A. P.; Karim, A.; Amis, E. J. Combinatorial Materials Science: Thin-Film Dewetting. *Macromolecules* **2000**, *33* (26), 9747–9756.

- (17) Sormana, J.-L.; Meredith, J. C. High-Throughput Discovery of Structure-Mechanical Property Relationships for Segmented Poly-(urethane-urea)s. *Macromolecules* **2004**, *37*, 2186–95.
- (18) Smith, A. P.; Douglas, J.; Meredith, J. C.; Karim, A.; Amis, E. J. High-Throughput Characterization of Pattern Formation in Symmetric Diblock Copolymer Films. *J. Polym. Sci., Part B: Polym. Phys.* **2001**, *39*, 2141–2158.
- (19) Liu, Y.; Hu, Z.; Suo, Z.; Hu, L.; Feng, L.; Gong, X.; Liu, Y.; Zhang, J. High-throughput experiments facilitate materials innovation: A review. *Sci. China: Technol. Sci.* **2019**, *62* (4), 521–545.
- (20) Potyrailo, R.; Rajan, K.; Stoewe, K.; Takeuchi, I.; Chisholm, B.; Lam, H. Combinatorial and High-Throughput Screening of Materials Libraries: Review of State of the Art. *ACS Comb. Sci.* **2011**, *13* (6), 579–633.
- (21) Green, M. L.; Choi, C. L.; Hatrick-Simpers, J. R.; Joshi, A. M.; Takeuchi, I.; Barron, S. C.; Campo, E.; Chiang, T.; Empedocles, S.; Gregoire, J. M.; Kusne, A. G.; Martin, J.; Mehta, A.; Persson, K.; Trautt, Z.; Van Duren, J.; Zakutayev, A. Fulfilling the promise of the materials genome initiative with high-throughput experimental methodologies. *Appl. Phys. Rev.* **2017**, *4* (1), 011105.
- (22) Shen, W. Characterization of mar/scratch resistance of polymer coatings: Part I. *JCT Coat. Tech.* **2006**, No. March, 54–60.
- (23) Wong, M.; Lim, G. T.; Moyses, A.; Reddy, J. N.; Sue, H. J. A new test methodology for evaluating scratch resistance of polymers. *Wear* **2004**, *256* (11–12), 1214–1227.
- (24) Burnett, P. J.; Rickerby, D. S. The Scratch Adhesion Test - an Elastic-Plastic Indentation Analysis. *Thin Solid Films* **1988**, *157* (2), 233–254.
- (25) Bull, S. J. Failure Modes in Scratch Adhesion Testing. *Surf. Coat. Technol.* **1991**, *50* (1), 25–32.
- (26) Bull, S. J. Failure mode maps in the thin film scratch adhesion test. *Tribol. Int.* **1997**, *30* (7), 491–498.
- (27) Kuo, T.-C.; Malvadkar, N. A.; Drumright, R.; Cesaretti, R.; Bishop, M. T. High-Throughput Industrial Coatings Research at The Dow Chemical Company. *ACS Comb. Sci.* **2016**, *18* (9), 507–526.
- (28) Ranjbar, Z.; Rastegar, S. Evaluation of mar/scratch resistance of a two component automotive clear coat via nano-indenter. *Prog. Org. Coat.* **2009**, *64* (4), 387–391.
- (29) Browning, R. L.; Lim, G. T.; Moyses, A.; Sue, H. J.; Chen, H.; Earls, J. D. Quantitative evaluation of scratch resistance of polymeric coatings based on a standardized progressive load scratch test. *Surf. Coat. Technol.* **2006**, *201* (6), 2970–2976.
- (30) Sormana, J. L.; Chattopadhyay, S.; Meredith, J. C. High-throughput mechanical characterization of free-standing polymer films. *Rev. Sci. Instrum.* **2005**, *76*, 062214.
- (31) Basak, P.; Zapata, P.; Reed, K.; Gomez, I.; Meredith, J. C. Continuous Infusion Microchannel Approach to Generate Composition Gradients from Viscous Polymer Solutions. In *Soft Matter Gradient Surfaces: Methods and Applications*; Genzer, J., Ed.; Wiley: New York, 2012; pp 129–143.
- (32) Coleman, M. M.; Lee, K. H.; Skrovanek, D. J.; Painter, P. C. Hydrogen-Bonding in Polymers 0.4. Infrared Temperature Studies of a Simple Polyurethane. *Macromolecules* **1986**, *19* (8), 2149–2157.
- (33) Wang, F. C.; Feve, M.; Lam, T. M.; Pascault, J. P. Ftir Analysis of Hydrogen-Bonding in Amorphous Linear Aromatic Polyurethanes 0.1. Influence of Temperature. *J. Polym. Sci., Part B: Polym. Phys.* **1994**, *32* (8), 1305–1313.
- (34) Luo, N.; Wang, D. N.; Ying, S. K. Hydrogen-bonding properties of segmented polyether poly(urethane urea) copolymer. *Macromolecules* **1997**, *30* (15), 4405–4409.